

Molecular field theory for biaxial smectic A liquid crystals

T.B.T. To,¹ T.J. Sluckin,^{1, a)} and G.R. Luckhurst²

¹*School of Mathematics, University of Southampton, Southampton, SO17 1BJ, United Kingdom*

²*School of Chemistry, University of Southampton, Southampton, SO17 1BJ, United Kingdom*

(Dated: 16 November 2021)

Thermotropic biaxial nematic phases seem to be rare, but biaxial smectic A phases less so. Here we use molecular field theory to study a simple two-parameter model, with one parameter promoting a biaxial phase and the second promoting smecticity. The theory combines the biaxial Maier-Saupe and McMillan models. We use alternatively the Sonnet-Virga-Durand (SVD) and geometric mean approximations (GMA) to characterize molecular biaxiality by a single parameter. For non-zero smecticity and biaxiality, the model always predicts a ground state biaxial smectic A phase. For a low degree of smectic order, the phase diagram is very rich, predicting uniaxial and biaxial nematic and smectic phases, with in addition a variety of tricritical and tetra-critical points. For higher degrees of smecticity, the region of stability of the biaxial nematic phase is restricted and eventually disappears, yielding to the biaxial smectic phase. Phase diagrams from the two alternative approximations for molecular biaxiality are similar, except inasmuch that SVD allows for a first order isotropic-nematic biaxial transition, whereas GMA predicts a Landau point separating isotropic and biaxial nematic phases. We speculate that the rarity of thermotropic biaxial nematic phases is partly a consequence of the presence of stabler analogous smectic phases.

PACS numbers: 64.70.M-, 61.30.Cz, 61.30.Eb

^{a)}Electronic mail: T.J.Sluckin@soton.ac.uk

I. INTRODUCTION

The possible existence of a biaxial nematic liquid crystal phase (N_B) was predicted over forty years ago by Freiser¹. In the intervening period the subject has been the focus of much intensive theoretical (e.g.²⁻⁴), computational (e.g.⁵) and experimental (see e.g.⁶⁻⁸) research. There are well-attested observations of lyotropic biaxial nematic phases⁹, but there has been considerable controversy over the well-publicized reports^{7,8} of the existence of thermotropic biaxial nematic phases (see e.g.¹⁰⁻¹²). It is by now clear that at the very least thermotropic biaxial nematic phases are rather rare.

Why this is the case is not entirely clear. Most nematogenic molecules are to some extent biaxial, and those explicitly constructed with a view to observing the biaxial nematic phase rather more so. One suggestion is that merely the temperature range over which the biaxial phase might be expected is rather narrow, while others have suggested that in lyotropics (but not in thermotropics), polydispersity might stabilize otherwise unstable phases¹³. However, these suggestions are difficult to evaluate, given the lack of suitable experimental points of reference.

However, one possibility with some experimental support is that biaxial nematogens are also suitably shaped so that they may also form smectic phases. The idea here is that the smectic biaxial phase SmA_B would in some sense destabilize the N_B phase (we also use the notations N_U, SmA_U, I to denote the uniaxial nematic, uniaxial smectic and isotropic liquid phases, respectively). The first suggestion of a biaxial smectic phase was made by de Gennes (see Teixeira *et al.*¹⁴). The first detailed theory was developed by Matsushita¹⁵, but his results have proved difficult to interpret in a more general context.

Experimentally, biaxial smectic phases are much less elusive than their nematic biaxial counterparts, giving some support to the intuitive idea of a competition between smectic and nematic biaxial stability. For example, non-polar biaxial smectic A phases have been discovered in a binary mixture of a board-like mesogen with a board like non-mesogenic compound^{16,17}, and in compounds of dimers of a rod-like and a bent-core mesogenic units^{18,19}. These experiments claim to find two phase sequences: $SmA_B - N_B - I$ ¹⁸ and $SmA_B - N_U - I$ ¹⁹. In addition, in a variety of different chemical contexts related biaxial smectic A phases with antiferroelectric order, usually denoted by SmA_{db} or SmA_dP_a , have also been observed²⁰⁻²⁴. In these materials, the phase sequence is always $SmA_{db} - SmA_U - I$.

In two experimental cases^{18,19}, the non-polar biaxial $\text{Sm}A_B$ phase is formed directly from the nematic phase on lowering temperature. Interestingly, the phase sequence $\text{Sm}A_B - N_U - I$ ¹⁹ has also been found theoretically in the Matsushita molecular field theory¹⁵, and also computationally, in a set of Gay-Berne simulations for orthogonal parallelepiped molecules which favour face-to-face interaction²⁵. Here the $\text{Sm}A_B$ is formed directly from N_U . By contrast, one might naively expect that an intermediate N_B phase would interpose itself between the $\text{Sm}A_B$ and the N_U phases. The lack of intermediate N_B gives further intuitive support to the idea that the $\text{Sm}A_B$ is preempting the N_B , and thus rendering it unobservable.

In this paper we seek to develop simple molecular criteria which control the relative stability of the N_B and $\text{Sm}A_B$. Our development builds on theories of the uniaxial smectic phase $\text{Sm}A_U$ and of the biaxial nematic phase N_B . The basic theory of the uniaxial smectic phase $\text{Sm}A_U$ is that of McMillan^{26,27}. In the current work, we also decouple the spatial modulations from the orientational distribution in the full density-orientational distribution function, following Kventzel *et al*²⁸. In order to provide a tractable theory, in our treatment of biaxiality, we reduce the number of parameters controlling the biaxiality from two to one. In order to include a generic set of phase diagrams, we employ two variants of this strategy; these have previously been used in the context of nematic biaxiality. The approximations are: the geometric mean approximation (GMA)²⁹, and the Sonnet-Virga-Durand approximation (SVD)³⁰. We explain these key approximations in greater detail below. Our theory also builds on previous work by Teixeira *et al*¹⁴, who have sought to establish simple criteria for the formation of biaxial smectic phases formed from board-like molecules.

The paper is organized as follows. In section II, we give a brief resume of previous theories of the smectic phase and of nematic biaxiality, emphasizing the key approximations we shall employ later. In section III, we then use these ideas to develop our present theoretical framework. In section IV, we present results from our calculations. Finally in section V we discuss the context in which our results should be understood.

II. THEORETICAL BACKGROUND

A. Basic material

In this paper, molecular orientation Ω is parameterized in terms of three Euler angles ψ, θ, ϕ which take their conventional meanings (polar angle θ and zenithal angles ψ, ϕ). The Euler angle ψ is only of interest in the specifically biaxial phases. We suppose constituent molecules to possess D_{2h} symmetry (i.e. that of an orthogonal parallelepiped). In some cases the molecules of interest possess other symmetries, such as, for example, the C_{2v} symmetry occurring in bent-core molecules. However, in the cases of interest the second order tensor invariants, the means of which provide the order parameters in the theory, are those given by the D_{2h} symmetry.

The underlying basic theory, on all of our work relies, is the Maier-Saupe theory of nematic ordering (see e.g. de Gennes and Prost³¹), for which the free energy per particle is given by:

$$A = k_B T \int_{\Omega} d\Omega f(\Omega) \ln 4\pi f(\Omega) - \frac{1}{2} \epsilon S^2, \quad (1)$$

where S is the nematic order parameter (discussed in more detail in eq.(7a) below), k_B denotes the Boltzmann constant, T is absolute temperature and ϵ sets the scale of the molecular anisotropic interaction.

In this paper, thermodynamic quantities, namely the free energy, internal energy, potentials of mean torque, distribution functions and partition functions are formulated per particle. In addition, the temperature and energy quantities are expressed in non-dimensional units. We denote T as the temperature, A as the free energy, U as the internal energy and $U(z, \Omega)$ as the potential of mean torque. We shall work, where possible, in non-dimensional quantities, given in terms of their physical quantities by

$$\begin{aligned} T^* &= \frac{k_B T}{\epsilon}; & A^* &= \frac{A}{\epsilon}; \\ U^* &= \frac{U}{\epsilon}; & U^*(z, \Omega) &= \frac{U(z, \Omega)}{\epsilon}, \end{aligned} \quad (2)$$

where $U^*(z, \Omega)$ is a potential of mean torque on a molecule with orientation Ω at point z .

Our theory of the $\text{Sm}A_B$ phase combines elements of standard theories of the uniaxial smectic phase $\text{Sm}A_U$ ^{26–28} and of the biaxial nematic phase N_B ^{2,3,29,30,32}. In order to make our work self-contained, in this section we give a brief account of these theories.

B. McMillan theory of smectics

The McMillan theory^{26,27} restricts itself to uniaxial (i.e. $D_{\infty h}$) molecules, for which the only relevant Euler angle is the polar angle θ . The smectic layer thickness d is given in this theory. There is no attempt at self-consistency in determining, for example, the thickness d in terms of moments of a full interparticle potential, although other theories^{33,34} do make this attempt. An extra simplifying element (see eq.(5) below) was introduced by Kventzel *et al*²⁸. There is a single non-dimensional parameter α which drives smectic order. Increasing α increases the smectic ordering temperature. A brief summary of the theory follows.

The orientational-translational densities are given by a function

$$\rho(z, \theta) = \bar{\rho} d F(z, \theta), \quad (3)$$

where $\bar{\rho}$ is the mean particle number density, and $F(z, \theta)$ is a normalized orientational-translational distribution function. We suppress the variables ψ and ϕ . The former has no meaning for a $D_{\infty h}$ particle. We integrate over the latter, which is in any case irrelevant as the distribution function is independent of ϕ . $F(z, \theta)$ is periodic in z with period d , and is independent of the transverse position within the layer. The normalization is such that

$$\int_0^\pi \sin \theta d\theta \int_0^d dz F(z, \theta) = 1. \quad (4)$$

The distribution function $F(z, \theta)$ is factorized into pure translational and pure orientational distribution functions, using an approximation introduced by Kventzel *et al*²⁸:

$$F(z, \theta) = f(\theta)g(z), \quad (5)$$

with $g(z) = g(z + d)$. This approximation in principle has only limited validity, but in practice has been used with a good degree of success (see e.g.^{35,36}). The functions $f(\theta)$ and $g(z)$ are each independently normalized:

$$\int_0^\pi \sin \theta d\theta f(\theta) = \int_0^d g(z) dz = 1 \quad (6)$$

There are three order parameters. These are:

(a) the orientational order parameter

$$\begin{aligned} S &= \langle P_2(\cos \theta) \rangle = \left\langle \frac{1}{2} (3 \cos^2 \theta - 1) \right\rangle \\ &= \int_0^\pi \sin \theta d\theta f(\theta) P_2(\cos \theta). \end{aligned} \quad (7a)$$

the usual order parameter entering the theory of nematics;

(b) the smectic density wave amplitude:

$$\tau = \left\langle \cos \left(\frac{2\pi z}{d} \right) \right\rangle = \int_0^d dz g(z) \cos \left(\frac{2\pi z}{d} \right). \quad (7b)$$

(c) the so-called mixed orientational-translational order parameter:

$$\begin{aligned} \sigma &= \left\langle P_2(\cos \theta) \cos \left(\frac{2\pi z}{d} \right) \right\rangle \\ &= \int_0^\pi \sin \theta d\theta \int_0^d dz F(z, \theta) P_2(\cos \theta) \cos \left(\frac{2\pi z}{d} \right). \end{aligned} \quad (7c)$$

The distribution function decoupling eq.(5) reduces the number of independent order parameters from three to two, with

$$\sigma = S\tau. \quad (8)$$

The Helmholtz free energy density relative to a disordered phase is expressed in non-dimensional units as

$$\begin{aligned} A^* &= T^* \int_0^\pi \sin \theta d\theta f(\theta) \ln (2f(\theta)) \\ &+ T^* \int_0^d dz g(z) \ln (dg(z)) - \frac{1}{2} (S^2 + \alpha S^2 \tau^2). \end{aligned} \quad (9)$$

The first term comes from orientational entropy, the second from translational entropy, the third from orientational energy, while only the last term is due to the energy advantage of smectic order. The factors of 2 and d in the entropy integrals are normalizing factors, as in the isotropic phase $f(\theta) = 1/2$ and $g(z) = d^{-1}$.

The key non-dimensional input parameter in the theory is α , with $0 \leq \alpha \leq 2^{26}$. The parameter α indicates the scale of the smectic ordering energy relative to that of the nematic ordering alone. We note that in this theory, high nematic ordering is required to induce smectic ordering, but the higher the value of α , the lower the required degree of nematic

order. An extra term $-\frac{1}{2}\delta\tau^2$ which would favor spontaneous smectic ordering in the absence of nematic ordering has been omitted (i.e $\delta = 0$)^{26,27}. Such a term could be reintroduced, for example, in a lamellar phase made from block copolymers, in which nematic order was induced by smectic order and not vice-versa, but we do not consider it here.

The distribution functions $f(\theta)$ and $g(z)$ are now determined self-consistently from the order parameters, angular functions and the smecticity parameter α ²⁸. They can be compactly written in terms of non-dimensionalized potentials of mean torque, $U_\theta^*(\theta)$ and $U_z^*(z)$, as

$$f(\theta) = Q_\theta^{-1} \exp \left[-\frac{U_\theta^*(\theta)}{T^*} \right]; \quad (10a)$$

$$g(z) = Q_z^{-1} \exp \left[-\frac{U_z^*(z)}{T^*} \right]. \quad (10b)$$

The potentials of mean torque are given by

$$U_\theta^*(\theta) = -(1 + \alpha\tau^2)SP_2(\cos \theta); \quad (11a)$$

$$U_z^*(z) = -\alpha S^2 \tau \cos \left(\frac{2\pi z}{d} \right). \quad (11b)$$

The partition functions Q_θ, Q_z are defined so as to normalize the distribution functions:

$$Q_\theta = \int_0^\pi \sin \theta d\theta \exp \left[\frac{-U_\theta^*(\theta)}{T^*} \right]; \quad (12a)$$

$$Q_z = \int_0^d dz \exp \left[\frac{-U_z^*(z)}{T^*} \right]; \quad (12b)$$

$$Q = Q_\theta Q_z. \quad (12c)$$

The equilibrium free energy can be rewritten as:

$$A^* = -T^* \log Q + (1/2)(S^2 + 3\alpha\tau^2 S^2), \quad (13)$$

which determines absolute phase stability if there is more than one equilibrium.

Fig. 1 shows the phase diagram for this theory in the (T^*, α) plane. The theory predicts I , N_u and SmA_u phases, with their relative stability tuned by varying α . Smectic order is favored (i.e. the onset of smectic order occurs at higher temperatures) with increasing α . For low α the $N_U - SmA_U$ transition is continuous, but it becomes first-order at a tricritical point at $\alpha = 0.52$. At a critical value of $\alpha = \alpha_c \approx 1.02$, the N phase disappears, and there

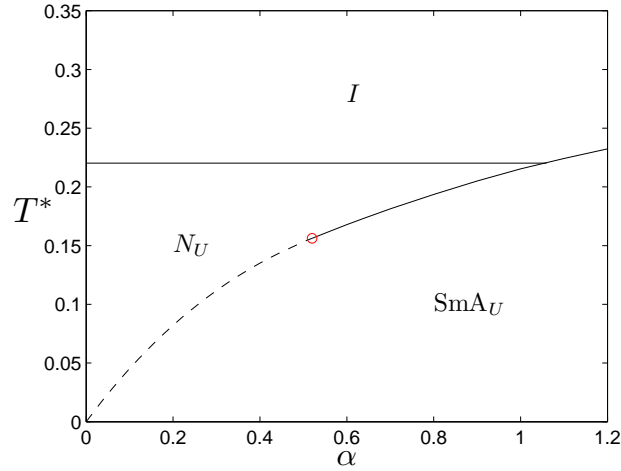


FIG. 1. Dependence of scaled transition temperature on smectic interaction parameter α , following Kventzel *et al*²⁸. Continuous lines: first order phase transitions; broken lines: continuous transitions; circle: $N_U - \text{Sm}A_U$ tricritical point.

is a direct $I - \text{Sm}A_U$ transition. A number of features of the theory are not robust, such as the temperature at three-phase coexistence, and the independence of T_{NI} of the smecticity parameter α . But the main general features of the phase diagram are conserved in more detailed theories and seem to correspond to experiment.

C. The biaxial nematic phase

The molecular field theory for D_{2h} biaxial nematics requires a normalized distribution function $f(\Omega)$, and four scalar order parameters (S, D, P, C) ^{4,32}, which are orientational averages of basis angular functions (R_S, R_D, R_P, R_C) . We follow the notation convention of Teixeira *et al*¹⁴, with different scaling. The functions are:

$$R_S(\Omega) = P_2(\cos \theta); \quad (14a)$$

$$R_D(\Omega) = \sqrt{3/8} \sin^2 \theta \cos 2\phi; \quad (14b)$$

$$R_P(\Omega) = \sqrt{3/8} \sin^2 \theta \cos 2\psi; \quad (14c)$$

$$R_C(\Omega) = (1/2) (1 + \cos^2 \theta) \cos 2\phi \cos 2\psi \\ - \cos \theta \sin 2\phi \sin 2\psi. \quad (14d)$$

The order parameters are defined in terms of basis angular function averages:

$$i = \langle R_i \rangle = \int_{\Omega} d\Omega f(\Omega) R_i(\Omega), \quad (15)$$

with $i \in \{S, D, P, C\}$. We note that (subject to exchange of axes) in the N_U phase, in general, $S, D \neq 0$, but $C = P = 0$. In biaxial phases all four order parameters in general are non-zero.

The degree of biaxiality is controlled by two parameters, (γ, λ) (see e.g.³⁰), which enter the non-dimensional internal energy as follows:

$$U_N^* = -\frac{1}{2} (S^2 + 4\gamma SD + 4\lambda D^2 + 2(P^2 + 2\gamma PC + \lambda C^2)). \quad (16)$$

The case $\lambda = \gamma = 0$ corresponds to uniaxial $D_{\infty h}$ molecules. The orientational distribution function $f(\Omega)$ is derived by minimizing a Helmholtz free energy functional:

$$A^* = -T^* \int_{\Omega} d\Omega f(\Omega) \ln (8\pi^2 f(\Omega)) + U_N^*. \quad (17)$$

The equilibrium orientational distribution function $f(\Omega)$ is expressed in term of the potential of mean torque

$$U_{\Omega}^*(\Omega) = -\left[(S + 2\gamma D)R_S(\Omega) + 2(\gamma S + 2\lambda D)R_D(\Omega) + 2(P + \gamma C)R_P(\Omega) + 2(\gamma P + \lambda C)R_C(\Omega) \right], \quad (18)$$

and is given by

$$f(\Omega) = Q_{\Omega}^{-1} \exp \left[-\frac{U_{\Omega}^*(\Omega)}{T^*} \right], \quad (19)$$

where the partition function Q_{Ω} is defined in order to normalise $f(\Omega)$:

$$Q_{\Omega} = \int_{\Omega} d\Omega \exp \left[-\frac{U_{\Omega}^*(\Omega)}{T^*} \right]. \quad (20)$$

The phase stability of the system is determined from the equilibrium Helmholtz free energy:

$$A^* = -T^* \log Q_{\Omega} + \frac{1}{2} \left(S^2 + 4\gamma SD + 4\lambda D^2 + 2(P^2 + 2\gamma PC + \lambda C^2) \right). \quad (21)$$

In general both γ, λ are required to define the full biaxiality. There are two particular limits which enable the biaxiality to be expressed in terms of a single parameter. We now discuss these in turn.

1. The geometric mean approximation (GMA)

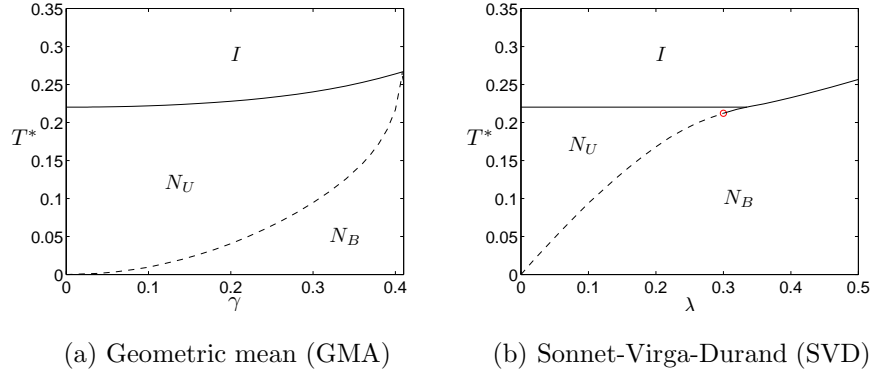


FIG. 2. Phase diagrams in biaxiality-temperature plane in the geometric mean (GMA) (a) and Sonnet-Virga-Durand (SVD) (b) approximations. Continuous lines: first order phase transitions; broken lines: continuous transitions; red circle: $N_U - N_B$ tricritical point.

The GMA limit $\gamma = \lambda^2$ emerges naturally from a consideration of dispersive forces or of geometric shapes^{2,3,29,30,32}. For a long time was regarded as generic. The interesting parameter range is $0 \leq \gamma \leq \gamma_c = \frac{1}{\sqrt{6}} \approx 0.408$. At γ_c , the biaxiality is in some sense maximal, and the roles of major and minor axes are exchanged, so that values of $\gamma > \gamma_c$ can be mapped onto values of $\gamma < \gamma_c$. Further discussion can be found e.g. in ref.[30]. The key feature of the resulting phase diagram is that there is a first-order $I - N_U$ phase transition, followed at a lower temperature by a continuous $N_U - N_B$ transition. These transitions collapse onto a single multicritical point (the Landau point) at $\gamma = \gamma_c$.

In the GMA, it can be shown, using eqs.(18,21), that the analysis requires only two order parameters, rather than the full complement of four. These are defined as follows:

$$\mathcal{J}_1 = \langle J_1(\Omega) \rangle = \langle R_S(\Omega) + 2\gamma R_D(\Omega) \rangle = S + 2\gamma D, \quad (22a)$$

$$\mathcal{J}_2 = \langle J_2(\Omega) \rangle = \langle R_P(\Omega) + \gamma R_C(\Omega) \rangle = P + \gamma C. \quad (22b)$$

In the I phase both order parameters are zero, in the N_U phase, $\mathcal{J}_1 \neq 0$, but $\mathcal{J}_2 = 0$, while in the N_B phase neither order parameter is zero.

2. The Sonnet-Virga-Durand approximation (SVD)

In this limit^{30,37} $\gamma = 0$. The relevant range is now $0 \leq \lambda \leq \frac{1}{2}$. In the SVD the so-called minor order parameters D and P identically vanish. Hence again there are only two order parameters, S, C , with $C = 0$ in the N_U phase.

There are two key differences between GMA and SVD. Firstly, in GMA, there is no direct $I - N_B$ transition except at a continuous transition at the single point of maximum biaxiality, usually known as the Landau multicritical point, where I, N_U, N_B coexist. By contrast, SVD predicts the whole line of first-order $N_B - I$ transitions. Secondly, GMA predicts that the $N_B - N_U$ transition is always continuous, whereas in SVD, the $N_B - N_U$ transition is continuous for a long range of biaxiality and first order for a small range of biaxiality, with a tricritical point on the $N_B - N_U$ transition line. Apart from this difference, the two phase diagrams are topologically similar, as can be seen in Figs.2, where we show the phase diagrams for GMA and SVD as functions of biaxiality and temperature.

III. MOLECULAR FIELD THEORY OF BIAxIAL SMECTIC PHASES.

A. Background

A formal derivation of the molecular field theory for biaxial smectic A phases, formed of molecules with D_{2h} symmetry, has been given by Teixeira *et al.*¹⁴. This is a combination of the molecular field theory for biaxial nematics and the McMillan theory for uniaxial smectic A. In addition, Teixeira *et al.*¹⁴ also discussed an alternative model based on the approximation by Kventzel, Luckhurst and Zewdie (KLZ)²⁸. In this section we discuss relevant equations for our calculation.

B. Distribution function and order parameters

As in section II B, the distribution function $F(z, \Omega)$ will be decoupled using the KLZ approximation²⁸, yielding $F(z, \Omega) = f(\Omega)g(z)$, with $\Omega = (\psi, \theta, \phi)$ as in sec. II C.

The principal order parameters are:

- (a) The biaxial nematic order parameters $i = \langle R_i \rangle$, for $i \in \{S, P, C, D\}$, as defined in eq.(15). As in section II C, we shall consider GMA and SVD flavors, which both reduce

this order parameter set to two independent parameters, one representing uniaxial order and one biaxial order.

(b) The simple smectic order parameter

$$\begin{aligned}
\tau &= \left\langle \cos \left(\frac{2\pi z}{d} \right) \right\rangle \\
&= \int_{\Omega} d\Omega \int_0^d dz F(z, \Omega) \cos \left(\frac{2\pi z}{d} \right) \\
&= \int_0^d dz g(z) \cos \left(\frac{2\pi z}{d} \right)
\end{aligned} \tag{23}$$

as in eq.(8), representing the magnitude of the density modulation. Note that we have used the decoupling approximation to eliminate the angular integral.

(c) The amplitudes of the periodic modulations the nematic order parameters, combining eqs.(7c,15):

$$\begin{aligned}
\sigma_i &= \left\langle \cos \left(\frac{2\pi z}{d} \right) R_i(\Omega) \right\rangle \\
&= \int_{\Omega} d\Omega \int_0^d dz F(z, \Omega) \cos \left(\frac{2\pi z}{d} \right) R_i(\Omega) \\
&= \int_{\Omega} d\Omega f(\Omega) R_i(\Omega) \int_0^d dz g(z) \cos \left(\frac{2\pi z}{d} \right) \\
&= \langle R_i \rangle \tau,
\end{aligned} \tag{24}$$

for $i \in \{S, P, C, D\}$.

C. Internal energy

The internal energy of the system consists of two parts: U_N^* and U_S^* , which can be associated respectively with purely nematic energy and a smectic contribution coming from orientational-translational coupling:

$$U^* = U_N^* + U_S^*. \tag{25}$$

The nematic free energy is as given in eq.(16)

$$U_N^* = -\frac{1}{2} \left(S^2 + 4\gamma SD + 4\lambda D^2 + 2(P^2 + 2\gamma PC + \lambda C^2) \right). \tag{26}$$

The second part of the internal energy is the mixed orientational-translational interaction, which we write by analogy with eqs.(9,16) as:

$$U_S^* = -\frac{1}{2}\alpha \left(\sigma_S^2 + 4\gamma'\sigma_S\sigma_D + 4\lambda'\sigma_D^2 + 2(\sigma_P^2 + 2\gamma'\sigma_P\sigma_C + \lambda'\sigma_C^2) \right). \quad (27)$$

In connection with the smectic contribution, we note that:

- (a) it is weighted by the same factor α (and for the same reason) as occurs in the McMillan theory eq.(9);
- (b) the molecules possess D_{2h} symmetry, and so the degree of biaxiality must be characterized by parameters γ', λ' which bear the same relationship to the smectic potential interaction as γ, λ do to the nematic biaxial interaction.

In order to simplify eq.(27):

- (i) we recall the distribution function decoupling result $\sigma_i = \langle R_i \rangle \tau$.
- (ii) we suppose $\gamma' = \gamma; \lambda' = \lambda$, yielding the following result for the mixed orientational-translational interaction energy:

$$U_S^* = -\frac{1}{2}\alpha\tau^2 \left(S^2 + 4\gamma SD + 4\lambda D^2 + 2(P^2 + 2\gamma PC + \lambda C^2) \right). \quad (28)$$

Finally, we note that in principle, a third contribution of form $U_0^* = -\frac{1}{2}\delta\tau^2$ is possible. We omit this term, partly for simplicity, partly because it refers to spontaneous layer formation, not driven by the orientational potential, and partly because we are concentrating on predicting trends. As discussed in sec.IIB, we shall neglect this term (i.e. $\delta = 0$). For detailed agreement with experimental results (e.g. see ref.[27]), it may be necessary to include it. Our final expression for the total internal energy is thus:

$$U^* = -\frac{1}{2}(1 + \alpha\tau^2) \left(S^2 + 4\gamma SD + 4\lambda D^2 + 2(P^2 + 2\gamma PC + \lambda C^2) \right) = -(1 + \alpha\tau^2) U_N^*. \quad (29)$$

D. Helmholtz free energy and potential of mean torque

The liquid crystalline contribution to Helmholtz free energy, per particle, is given by

$$A^* = T^* \int_{\Omega} d\Omega f(\Omega) \ln \left(8\pi^2 f(\Omega) \right) + T^* \int_0^d dz g(z) \ln \left(dg(z) \right) + (1 + \alpha\tau^2) U_N^*. \quad (30)$$

We note that in eq.(30), as is usual in liquid crystal calculations, the isotropic phase contribution to the Helmholtz free energy has been subtracted. Thus in the isotropic limit, in which $f(\Omega) = \frac{1}{8\pi^2}$; $g(z) = \frac{1}{d}$, $A^* = 0$.

The orientational and translational distribution functions can be determined by minimizing the free energy given in eq.(30) and can be written compactly in terms of the potentials of mean torque as

$$f(\Omega) = Q_{\Omega}^{-1} \exp \left[-\frac{U_{\Omega}^*(\Omega)}{T^*} \right]; \quad (31a)$$

$$g(z) = Q_z^{-1} \exp \left[-\frac{U_z^*(z)}{T^*} \right], \quad (31b)$$

where the potentials of mean torque are given by

$$U_{\Omega}^*(\Omega) = -(1 + \alpha\tau^2) \left[(S + 2\gamma D) R_S(\Omega) + 2(\gamma S + 2\lambda D) R_D(\Omega) + 2(P + \gamma C) R_P(\Omega) + 2(\gamma P + \lambda C) R_C(\Omega) \right]; \quad (32)$$

$$U_z^*(z) = -2\alpha\tau U_N^* \cos(2\pi z/d). \quad (33)$$

The partition functions Q_{Ω}, Q_z are defined so as to normalize the distribution functions:

$$Q_{\Omega} = \int_{\Omega} d\Omega \exp \left[\frac{-U_{\Omega}^*(\Omega)}{T^*} \right]; \quad (34a)$$

$$Q_z = \int_0^d dz \exp \left[\frac{-U_z^*(z)}{T^*} \right]; \quad (34b)$$

$$Q = Q_{\Omega} Q_z. \quad (34c)$$

At a given temperature, the value of the free energy at an equilibrium point is given by

$$A^* = -T^* \log Q + (1 + 3\alpha\tau^2) U_N^*. \quad (35)$$

In subsections II C 1 and II C 2, we have discussed the geometric mean (GMA) and Sonnet-Virga-Durand (SVD) approximations, which we now use in our biaxial smectic A phase calculation. We recall that these approximations enable the internal energy (here eq. (26)), and the orientational potential of mean torque (here eq. (32)) to be rewritten compactly in terms of only two order parameters, controlled by a single biaxiality parameter.

- (a) **GMA:** The two independent composite orientational order parameters have been given in eqs. (22a,22b), and are \mathcal{J}_1 (non-zero in all liquid crystal phases) and \mathcal{J}_2 (only non-zero in biaxial phases). The nematic internal energy and potential of mean torque in eqs. (26) and (32) can be rewritten compactly in terms of $\mathcal{J}_1, \mathcal{J}_2$

$$U_N^* = -\frac{1}{2}(\mathcal{J}_1^2 + 2\mathcal{J}_2^2); \quad (36)$$

$$U_\Omega^*(\Omega) = -(1 + \alpha\tau^2)\left(\mathcal{J}_1 J_1(\Omega) + 2\mathcal{J}_2 J_2(\Omega)\right). \quad (37)$$

Thus in this model, there are three self-consistency equations, given by eq. (23) and

$$\mathcal{J}_i = \int_{\Omega} d\Omega f(\Omega) J_i(\Omega), \quad (38)$$

with $i \in \{1, 2\}$.

- (b) **SVD:** The two orientational order parameters are S (non-zero in all liquid crystal phases) and C (only non-zero in biaxial phases). The nematic internal energy and potential of mean torque in eqs. (26) and (32) can be rewritten compactly in terms of S, C

$$U_N^* = -\frac{1}{2}(S^2 + 2\lambda C^2); \quad (39)$$

$$U_\Omega^*(\Omega) = -(1 + \alpha\tau^2)\left(S R_S(\Omega) + 2\lambda C R_C(\Omega)\right). \quad (40)$$

Thus in this model, there are three self-consistency equations, given by eq. (23) and

$$i = \langle R_i \rangle = \int_{\Omega} d\Omega f(\Omega) R_i(\Omega), \quad (41)$$

with $i \in \{S, C\}$.

E. Method

The procedure to determine the stable state at a given temperature involves solving the relevant self-consistent equations for both the GMA and the SVD models. In each case

we solve the three self-consistency equations, eqs.(23, 38) for GMA and (23,41) for SVD, using the MATLAB function *fsolve*. This function uses an improved Newton’s method (the so-called trust-region dogleg algorithm) and iterates towards a solution from a given starting point. The chosen solution is the one that give the lowest value for the free energy in eq. (35). A phase transition occurs at the point at which one or more order parameters change from a zero to a non-zero value as the temperature is lowered.

IV. NUMERICAL RESULTS

We present results from both the GMA and SVD flavors of our theory, and then discuss what features these two sets of results possess in common.

A. GMA

In Figs.3 we show a representative set of five GMA phase diagrams for increasing α . Each phase diagram shows a constant α slice in the $(\alpha - \gamma - T^*)$ space. All topological configurations of phases that we find are shown in one of these examples. We recall that in zero smecticity case ($\alpha = 0$) the stability of the biaxial nematic phase N_B increases relative that of the uniaxial nematic N_U on increasing γ , up to the Landau multicritical point at $\gamma = \gamma_c = \frac{1}{\sqrt{6}}$. Symmetry around γ_c then implies that the same series of phases occurs for $\gamma \geq \gamma_c$ as for $\gamma \leq \gamma_c$. We expect this symmetry also to apply for non-zero α , and our pictures only include the cases $\gamma \leq \gamma_c$.

For completeness, we include in Figs.3 the zero smecticity case $\alpha = 0$ phase diagram, already discussed in section II C (see Fig.2a). Here, except at $\gamma = 0$, the ground state is always N_B . For low γ , the N_B phase only intercedes at very low temperatures. Only for γ very close to γ_c does the $N_U - N_B$ phase boundary noticeably increase in temperature. Then at the Landau multicritical point $\gamma = \gamma_c$, all phases coincide.

For $\alpha = 0.3$, shown in Fig.3b, the higher temperature part of this diagram ($T^* \gtrsim 0.1$) is unchanged from the $\alpha = 0$ case, indicating that the orientational-translational coupling is sufficiently low that low temperatures are required to activate the smectic modulation. But now at sufficiently low temperatures both uniaxial SmA_U and biaxial smectic SmA_B phases are stabilized, with the stability of the SmA_B phase increasing significantly at larger γ .

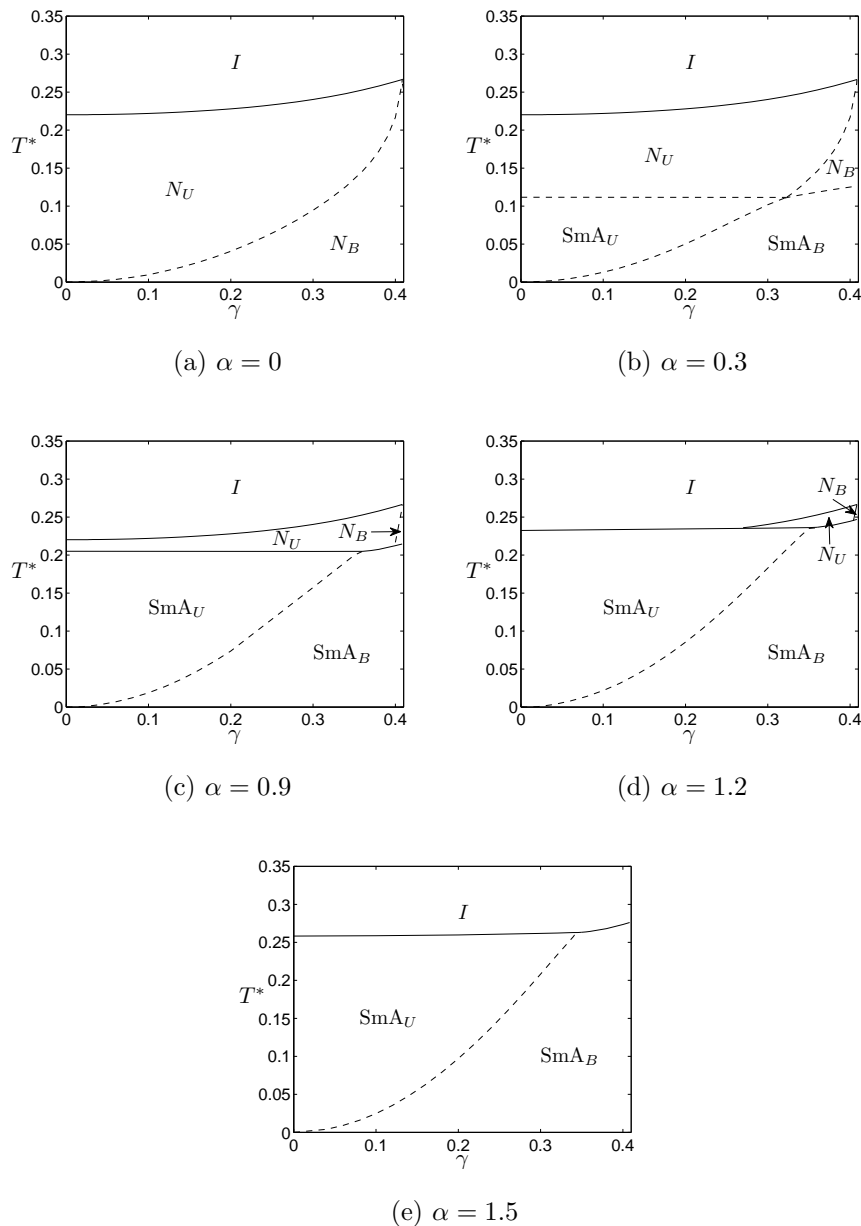


FIG. 3. Geometric mean approximation phase diagrams as a function of biaxiality γ and scaled temperature T^* , for representative values of the McMillan smectic parameter α . Continuous lines: first order phase transitions; broken lines: continuous transitions.

The ground state N_B phase is unsurprisingly preempted by a SmA_B phase, while for values of γ for which the N_B phase requires very low temperatures, the N_U phase yields to a SmA_U phase. This picture seems generic for low positive α . Although the N_U and even N_B phases are retained at higher temperatures, the N_B phase is now confined to a window around

the Landau multicritical point. In the $\alpha = 0.3$ case, this corresponds to $T^* \gtrsim 0.5T_{NI}$, and $0.32 \lesssim \gamma \lesssim 0.41$. The temperature at the $N_U - \text{Sm}A_U$ phase boundary is independent of α , and the transition is continuous. Likewise the $N_U - N_B$ transition remains continuous at finite α , as are the new $N_B - \text{Sm}A_B$ and $\text{Sm}A_U - \text{Sm}A_B$ transitions. An interesting, if implausible, stable feature of this phase diagram is a four-phase coexistence point at $\gamma \approx 0.32, T^* \approx 0.11$, at which the three continuous phase transition lines $N_U - N_B$, $N_U - \text{Sm}A_U$, $\text{Sm}A_U - \text{Sm}A_B$ collide.

For $\alpha = 0.9$ (see Fig.3c), the stability region of the nematic phases is much smaller. In addition, the $\text{Sm}A_U - N_U$ transition is now first order, consistent with the $\gamma = 0$ phase diagram in Fig.1. As in the $\alpha = 0.3$ case, the $\text{Sm}A_B$ phase is increasingly stable at higher γ . The $\text{Sm}A_B - \text{Sm}A_U$ transition is still second order, but now the $\text{Sm}A_B - N_B$ and $\text{Sm}A_B - N_U$ transitions are first order. We note also that the $\alpha = 0.3$ four-phase $N_U, N_B, \text{Sm}A_U, \text{Sm}A_B$ coexistence point has split into two separate critical end points, one for $N_U, \text{Sm}A_U, \text{Sm}A_B$ and one for $N_U, N_B, \text{Sm}A_B$. The already narrow N_B stability has shrunk further, and is now just a sliver for $0.4 \lesssim \gamma \lesssim 0.41$, and (at its greatest) $T^*/T_{NI}^* \gtrsim 0.85$.

For $\alpha = 1.2$ (see Fig.3d), the N_U phase is pre-empted by the $\text{Sm}A_U$ phase over most of its range, and the $I - N_U$ transition line is replaced by a line of direct $I - \text{Sm}A_U$ transitions. This feature of the phase diagram is consistent with the smectic molecular field theory²⁸, shown in Fig. 1 for $\gamma = 0$. The nematic phase region is now confined to a narrow temperature range close to the Landau multicritical point; N_B phase is just hanging on in a tiny region in the immediate neighborhood of the Landau multicritical point.

In the the final case we consider, $\alpha = 1.5$ (see Fig. 3e), the orientational-translational coupling is now large enough to induce smectic order as soon as nematic order appears. Now the narrow regions of N_U, N_B stability have both been overtaken by smectic order. For $\gamma \lesssim 0.34$, there is a direct $\text{Sm}A_U - I$ phase transition, while for $0.34 \lesssim \gamma \lesssim \gamma_c \approx 0.41$, there is a direct $\text{Sm}A_B - I$ phase transition line. At lower temperatures for all $\gamma \lesssim 0.34$, there is a further continuous $\text{Sm}A_U - \text{Sm}A_B$ transition.

Finally in Fig.4, we summarize these results, showing the phase sequences which occur, as a function of the two control parameters γ, α . We postpone a detailed discussion of this diagram. However, we can note immediately there are five predicted phase sequences. But only one out of these five – the shaded region **B** in Fig.4 – includes the biaxial nematic N_B . and this is a rather restricted region of the control parameter plane.

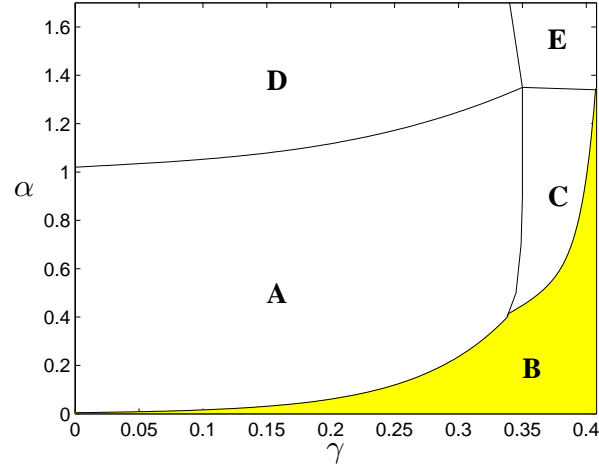


FIG. 4. GMA: phase sequences observed (approximate) in the (γ, α) (biaxiality-smecticity) plane. The region with stabilized N_B is shaded (yellow online).

A: $\text{Sm}A_B - \text{Sm}A_U - N_U - I$ **B:** $\text{Sm}A_B - N_B - N_U - I$

C: $\text{Sm}A_B - N_U - I$ **D:** $\text{Sm}A_B - \text{Sm}A_U - I$

E: $\text{Sm}A_B - I$

B. SVD

In Figs.5 we show a representative set of four SVD phase diagrams for increasing α . Each phase diagram shows a constant α slice in the $(\alpha - \lambda - T^*)$ space. As in the GMA case, all topological configurations of phases that we find are shown in one of these examples. We recall that in zero smecticity case ($\alpha = 0$) the biaxiality parameter is restricted to $0 \leq \lambda \leq 0.5$.

For completeness, we include in Fig.5a the zero smecticity case $\alpha = 0$ phase diagram, already discussed in section IIC (see Fig.2b). Here, except at $\lambda = 0$, the ground state is always N_B . For small λ , the N_B phase occurs at very low temperatures. The stability of N_B gradually increases relative to that of N_U on increasing λ , up to the triple point $\lambda \approx 0.33$, where all phases coexist. The tricritical point at $\lambda \approx 0.3$ separates the first-order and continuous sections of the $N_B - N_U$ transition line. For $\lambda \gtrsim 0.33$, a single first order $N_B - I$ transition replaces the phase sequence $N_B - N_U - I$.

For $\alpha = 0.3$ (see Fig.5b) contains several features reminiscent of the GMA case. Indeed,

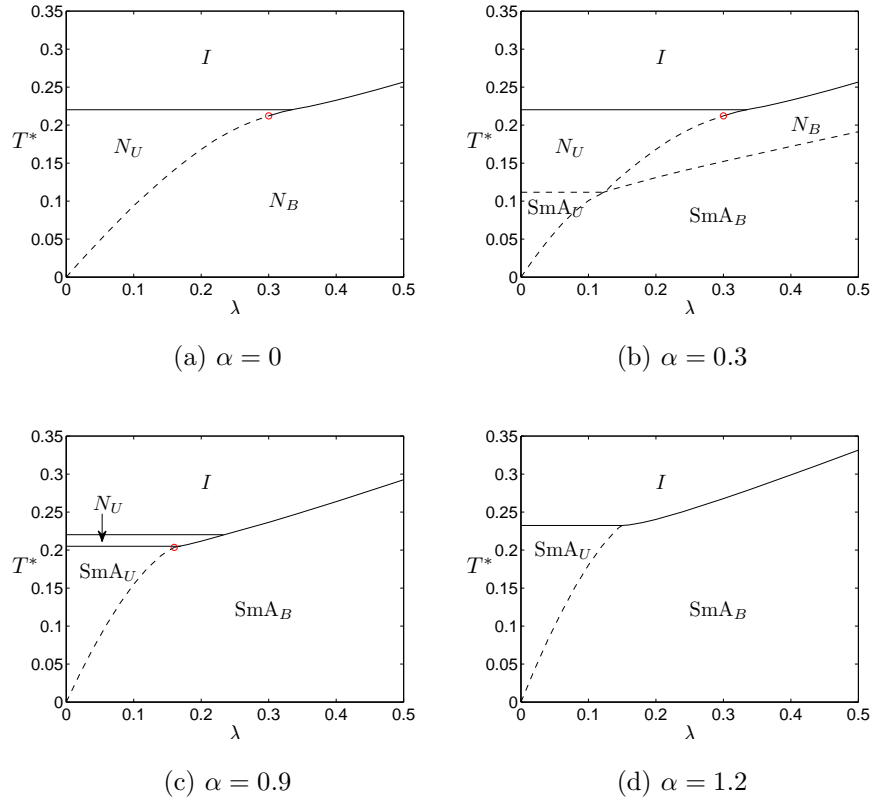


FIG. 5. SVD approximation phase diagrams as a function of biaxiality γ and scaled temperature T^* , for representative values of the McMillan smectic parameter α . Continuous lines: first order phase transitions; broken lines: continuous transitions; red circle: tricritical point.

the topological structure of this phase diagram is very similar to its GMA counterpart in Fig.3b. The main distinction is that here there is a line of first order $N_B - I$ transitions, which has shrunk in the GMA case to a single point.

Specifically, the high temperature part of this diagram ($T^* \gtrsim 0.2$) is unchanged from the $\alpha = 0$ case. The orientational-translational coupling is still too weak to turn on the smectic modulation. Likewise, at sufficiently low temperatures, both uniaxial $\text{Sm}A_U$ and biaxial smectic $\text{Sm}A_B$ phases are stabilized, with the stability of the $\text{Sm}A_B$ increasing gradually at larger λ . The ground state N_B is again replaced by $\text{Sm}A_B$, while for values of λ for which the N_B phase requires low temperatures, the N_U phase again yields to a $\text{Sm}A_U$ phase. This picture again seems generic for low positive α . The N_B phase has been restricted to a smaller range of $0.13 \lesssim \lambda \lesssim 0.5$. The temperature at the $N_U - \text{Sm}A_U$ phase boundary remains independent of α , and the transition is continuous. Likewise, the $N_U - N_B$ transition

remains continuous for $0.13 \lesssim \lambda \lesssim 0.3$, as are the new $N_B - \text{Sm}A_B$ and $\text{Sm}A_U - \text{Sm}A_B$. Finally, as in the GMA case, there is a four-phase coexistence point at $\lambda \approx 0.13, T^* \approx 0.12$, at which the three continuous phase transition lines $N_U - N_B, N_U - \text{Sm}A_U, \text{Sm}A_U - \text{Sm}A_B$ collide.

For $\alpha = 0.9$ (see Fig.5c), whereas in the GMA case, there still remained a thin region of N_B stability, here the region of N_B has been entirely overtaken by $\text{Sm}A_B$. The stability region of N_U is reduced into a narrow stripe at $T^* \approx 0.2$. The $\text{Sm}A_U - N_U$ transition is now first order, consistent with the $\lambda = 0$ phase diagram in Fig.1. As in the $\alpha = 0.3$ case, the $\text{Sm}A_B$ phase is increasingly stable at higher λ . A tricritical point at $\lambda \approx 0.16$ separates the first-order and continuous regions of the $\text{Sm}A_B - \text{Sm}A_U$ boundary line, although the first order section of this line is very short. The point of contact $\text{Sm}A_B - N_U$ at $\alpha = 0.3$ is now transformed into a first order transition line for $0.17 \lesssim \lambda \lesssim 0.23$, followed by the new first-order $\text{Sm}A_B - I$ transition line for $0.23 \lesssim \lambda \lesssim 0.5$.

In the final case we consider, $\alpha = 1.2$ (see Fig.5d), the entire nematic region has now been replaced by smectic phases. The $N_U - I$ transition line is replaced by a line of direct first-order $\text{Sm}A_U - I$ transitions for $0 \leq \lambda \lesssim 0.15$. This feature of the phase diagram is consistent with the smectic molecular field theory²⁸, shown in Fig. 1 for $\lambda = 0$. This $\text{Sm}A_U - I$ transition is followed by a continuous $\text{Sm}A_B - \text{Sm}A_U$ transition at a lower temperature. This phase sequence is also identical to that in the GMA case for $\alpha = 1.5$ (Fig.3e)

Fig.6 summarizes these results, showing the phase sequences as a function of the two control parameters λ, α . There are now six predicted phase sequences. Five are as in the GMA case (shaded regions *A* through *E*). Only two shaded regions, **B** and the new **F**), permit a biaxial nematic N_B , and these regions are restricted to a narrow region of the control parameter plane.

V. DISCUSSION

We have developed a family of simplified two-parameter molecular field theories, which allow for both smectic and biaxial nematic phases. The theories extend and combine standard models involving, on the one hand uniaxial nematic and smectic phases, and on the other hand uniaxial and biaxial nematics. We first discuss the approximations we have made.

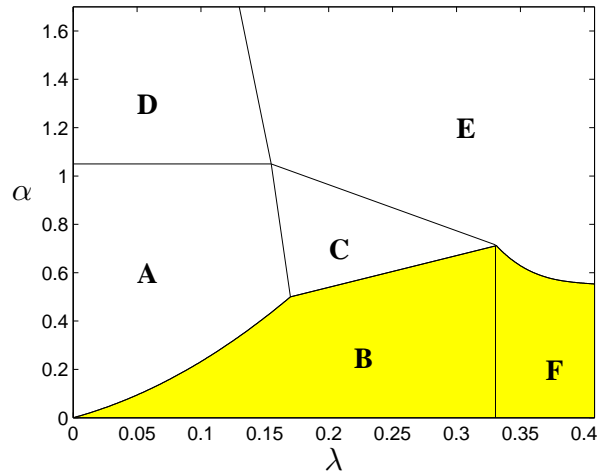


FIG. 6. SVD: phase sequences observed (approximate) in the (λ, α) (biaxiality-smecticity) plane.

The regions with stabilized N_B are shaded (yellow online).

- | | |
|---|---|
| A: $\text{Sm}A_B - \text{Sm}A_U - N_U - I$ | B: $\text{Sm}A_B - N_B - N_U - I$ |
| C: $\text{Sm}A_B - N_U - I$ | D: $\text{Sm}A_B - \text{Sm}A_U - I$ |
| E: $\text{Sm}A_B - I$ | F: $\text{Sm}A_B - N_B - I$ |

The phase diagrams corresponding to the nematic limits of these models are slightly different. The geometric mean approximation (GMA) uses a Lorentz-Berthelot combination rule to reduce the number of molecular biaxiality parameters, and seems to correspond to model interaction potentials between some simple model slab-like molecules. The Sonnet-Virga-Durand parameterization is easier to use mathematically, but harder to justify physically, except in the case of molecules of complicated shape. In the former case, in the pure nematic limit, there is a single Landau multicritical point at which the uniaxial and biaxial nematic states touch the isotropic phase. In the latter case in the nematic limit there is a line of first order isotropic-biaxial nematic transitions. Luckily, however, more general theoretical studies^{38,39} suggest strongly that one-parameter slices through general nematic biaxiality phase diagrams always give rise to phase portraits which possess the same topology as one of our approximations (i.e. one of the diagrams shown in Fig. 2).

The uniaxial smectic limit of this model involves the KLZ decoupling approximation²⁸, in which the molecular orientational distribution function is independent of position. Although this approximation cannot be completely accurate, it has great mathematical simplifying

power. The main topological features of the phase diagram – in particular the passage from a continuous to a first-order nematic-smectic transition with increasing translational-orientational coupling α , followed by the elimination of the nematic phase at still higher α – are correctly captured. In some cases^{40,41}, simulation of a model system has shown good agreement with this ansatz, while recent atomic simulations of 8CB, on the other hand, show that there are circumstances when this ansatz fails⁴².

In this paper we seek general explanations, rather than close numerical agreement with phase diagrams and thermodynamics in particular cases. The starting points for the models we have used in this paper are extremely simple. For our purposes they seem sufficiently well-founded.

The topologies of the phase diagrams predicted by our two zero-smecticity nematic approximation do differ. But nevertheless, subject to this proviso, the resulting emergent smectic biaxial phase diagrams do carry many features in common. For low values of the smectic parameter α , the uniaxial and biaxial nematic phases retain their integrity, but lower temperature phases are uniaxial and biaxial smectics; the ground state is always biaxial smectic. For higher values α , the nematic phases, and in particular the biaxial nematic phase, are restricted to very narrow regions of the phase diagram, and eventually squeezed out altogether.

A number of phase progressions have been predicted. The low smecticity $I - N_U - N_B$ (with decreasing temperature) gives way to $I - N_U - N_B - \text{Sm}A_B$ or $I - N_U - \text{Sm}A_U - \text{Sm}A_B$. The progression from the uniaxial nematic to the biaxial smectic seems to pass through either the biaxial nematic or the uniaxial smectic, but never both. The SVD approximation permits a direct first-order $I - N_B$ at low α , and hence a direct $I - N_B - \text{Sm}A_B$ transition at higher α . But of the predicted phase progressions, only the $I - N_B - \text{Sm}A_B$ progression does not occur in the simple geometric mean approximation. As α is further increased, the nematic phases progressively disappear. In this regime, for higher biaxiality we predict a direct $I - \text{Sm}A_B$ transition, while for lower biaxiality we expect the more indirect $I - \text{Sm}A_U - \text{Sm}A_B$ progression.

The set of phase progressions have been summarized in Figs. 4 and 6 for the GMA and the SVD respectively. Here the six possible phase orderings found in our theory are shown in the biaxiality-smecticity plane. The topological features of these diagrams are very similar. High smecticity and low biaxiality together predict the $I - \text{Sm}A_U - \text{Sm}A_B$ progression (regions

D in these figures). A lower degree of smecticity (regions A) allows the uniaxial nematic to intrude: $I - N_U - \text{Sm}A_U - \text{Sm}A_B$. High biaxiality and high smecticity (regions E) predict a direct $I - \text{Sm}A_B$ transition; now only the isotropic and biaxial smectic phases are allowed and all others have been squeezed out. For intermediate values of both parameters (regions C), our results predict that there will be a region in which there is a direct transition from the uniaxial nematic to the biaxial smectic ($I - N_U - \text{Sm}A_B$). Both approximation schemes allow for a low biaxiality, low smecticity regime (region B) in which a biaxial nematic intrudes between the uniaxial nematic and the biaxial smectic ($I - N_U - N_B - \text{Sm}A_B$). The SVD approximation alone predicts a further region F , for low smecticity and high biaxiality, in which the biaxial nematic occurs between the biaxial smectic and the isotropic phases: $I - N_B - \text{Sm}A_B$.

Of the six possible phase progressions, only two (regions B , common to both approximations, and region F occurring only in the SVD approximation) include the N_B phase. In each case these regions cover a relatively small proportion of the phase space. In addition, in the SVD case, where region B extends into a region of low biaxiality, the biaxial nematic phase occurs at low temperatures and would surely be pre-empted by a crystalline phase. The hypothesis that biaxial nematic phases are at least to some extent preempted by biaxial smectics thus seems to receive considerable informal support from Figs. 4 and 6.

Some more specific contact with experiment can be made as follows. Approximate values for parameters α and γ can be derived for a series of rigid bent-core molecule biaxial smectic A phases^{22,23}. For α , we use an argument due to McMillan²⁶, and for γ , we use an argument due to Ferrarini *et al*^{43,44}.

McMillan²⁶ proposed the following relation linking α , the length r_0 of a mesogenic unit in a smectogenic molecule, and the smectic layer spacing d :

$$\alpha = 2 \exp - \left(\frac{\pi r_0}{d} \right)^2, \quad (42)$$

Eq.(42) can now be inverted, yielding

$$\frac{d}{r_0} = \frac{\pi}{\sqrt{\ln 2 - \ln \alpha}}. \quad (43)$$

This gives the dependence of period spacing d on α . We now further suppose the smectic spacing d to be proportional to flexible chain length. It is now possible to make contact with experiments, in which phase maps are constructed in a $T - n$ plane, where $n \sim d$ is flexible chain length.

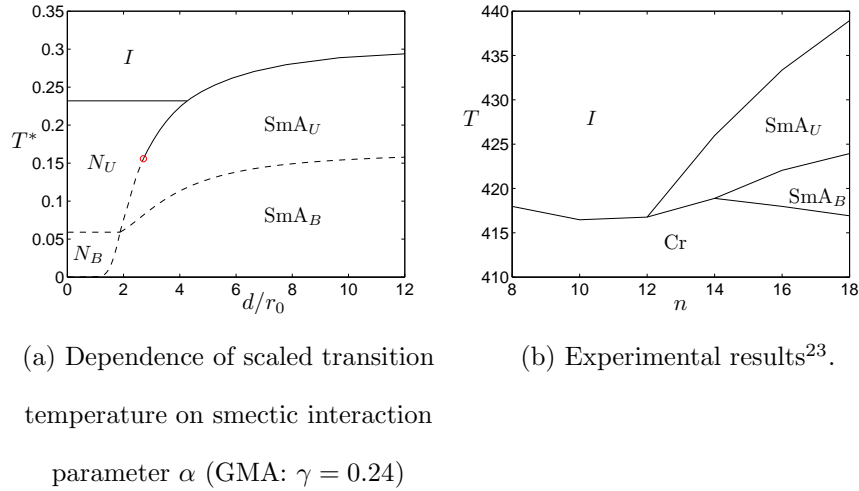


FIG. 7. (b): Dependence of transition temperature on number of carbon atoms in the flexible chain of a bent-core molecule, after ref. [23]. Antiferroelectric SmA_d is uniaxial; $\text{SmA}_d P_A$ is biaxial, Cr : crystal.

In the GMA, the biaxiality parameter γ has been related to the interarm angle of bent-core molecules^{43,44} by the following equation:

$$\gamma = \sqrt{\frac{3}{2}} \left(\frac{1 + \cos \theta}{1 - 3 \cos \theta} \right). \quad (44)$$

The chemical structure of the compound used in the experiments by Sadashiva *et al*²³ suggests an interarm angle of 120° , implying $\gamma \approx 0.24$. Thus, within the GMA, we can calculate a phase map for $\gamma = 0.24$ as a function of T^* and d/r_0 . We show this phase diagram in Fig.7, together with the experimental results by Sadashiva *et al*²³.

The details of the theoretical and observed phase maps differ. We note in particular that although the N_U phase is absent in the experiments, it appears in the phase maps. On the other hand, however, some features of the two phase maps resemble each other. Specifically, both the biaxial smectic A-to-uniaxial smectic A and uniaxial smectic A-to-isotropic phase transition temperatures increase with the number of carbon atoms in the flexible chain. Likewise, both these phase transition temperatures increase with the parameter α in the molecular field theory.

On the other hand, in the experiments, the onset of SmA_B occurs at much higher temperatures than the naive theory predicts. This may be because in the experiment, the smectic biaxial phase possesses a bilayer layer structure, and also possesses antiferroelectric order.

In addition, the molecules have dipolar shape. Thus transverse dipolar interaction may have stabilized the biaxial smectic phase. Future work, explicitly including antiferroelectric order, may resolve this point.

The smectic parameter α for uniaxial systems can be estimated by comparing results for $T_{\text{Sm}A_U N_U} / T_{N_U I}$ with experimental data of two calamitic series $n\text{CB}$? and $\bar{n}\text{S5}$?, where n is the number of Carbon atoms in the flexible chain. The phase sequence $\text{Sm}A_U - N_U - I$ occurs for $n = 8, 9$ for $n\text{CB}$ and $n = 8, 9, 10$ for $\bar{n}\text{S5}$. The estimated value of α for 8CB and $\bar{8}\text{S5}$ are 1.02 and 0.92, respectively. These calamitic molecules can be interpreted in the GMA model as having γ close to zero. From Fig.4 we see that the molecules 8CB and $\bar{8}\text{S5}$ are in region **A** of the parameter space.

We can also estimate α for shorter chain length. Using Eq.(43) and supposing that $d/r_0 = Cn$, we found that C decreases with n for both $n\text{CB}$ and $\bar{n}\text{S5}$ series; and this value for $\bar{n}\text{S5}$ is slightly smaller than $n\text{CB}$ with the same n . Thus, we use $C = 0.45$ (for $\bar{8}\text{S5}$) as the lower bound for smaller n for a general calamitic molecule. Thus for the shortest chain length for which a nematic phase exists $n = 5$, the estimated value for α , given by Eq.(42) is 0.28, which is clearly still in region **A** in Fig.4. Note that for this value of α to fall into the region with stabilized N_B , we need $0.3 \lesssim \gamma \leq 1/\sqrt{6}$. This is a rather high degree of biaxiality, and for higher n , the biaxial nematic region would be further restricted. By way of example, in the case of symmetric bent-core molecules with $n = 5$, using eq.(44), an interarm angle of $109.47^\circ \leq \gamma \lesssim 115^\circ$ would be required to stabilize the N_B phase.

We also note that some features of our results may not be generic, and may not persist when the KLZ decoupling approximation is relaxed. Some examples are:

- (a) Both Figs.3 and 5 include what seem to be exceptional points of four-phase contact ($N_U - N_B - \text{Sm}A_U - \text{Sm}A_B$), where the continuous $N_U - N_B$ and $N_U - \text{Sm}A_U$ lines collide. The fate of these points when the molecular field approximations include better chemical detail, or if fluctuations are included, is not clear.
- (b) In the present theory, the $N_U - \text{Sm}A_U$ tricritical lines appear in phase map slices in the smecticity-temperature plane, but do not appear in the Figs.3 and 5, which present phase map slices in the biaxiality-temperature plane. Presumably in more accurate theories, the tricritical points would be visible in both sets of slices.
- (c) In the phase progression maps, Figs 4 and 6, both include points where four sets of

phase progressions touch. One would not normally expect three lines in a picture to collide at a single point, although there may be thermodynamic reasons why this cannot be avoided.

In summary, we have developed a molecular field theory for biaxial smectic A phase by combining McMillan theory for uniaxial smectic A phases²⁶ and a generalized version of Straley theory³² for biaxial nematics. By applying several approximations, the number of input parameters in the model is restricted to a single degree of smecticity and a single degree of molecular biaxiality. Likewise, the number of order parameters is reduced from nine to three.

Numerical results show that the stability of smectic A phases increase on increasing the smectic interaction α . A system with high α and small biaxiality can still form a biaxial smectic A phase at high temperature. In contrast, for the same biaxiality, a system with low smectic interaction forms a biaxial nematic phase only at unphysically low temperatures. Our results also agree with empirical evidence that the stability of the biaxial and uniaxial smectic A phases increases with flexible chain length. On the basis of this study, we conclude that, with the same molecular biaxiality, macroscopic biaxial ordering is easier to form in the smectic A phases than in the nematic phases.

ACKNOWLEDGMENTS

TBTT acknowledges financial support of a School Ph.D. Studentship from the School of Mathematical Sciences, University of Southampton. We thank E.G. Virga, O.D. Lavrentovich, M.A. Osipov, I.I. Smalyukh and P.I.C. Teixeira for helpful discussions. TJS and TBTT thank the Isaac Newton Institute for Mathematical Sciences, University of Cambridge, for hospitality while some of the final parts of this research were carried out.

REFERENCES

- ¹M. J. Freiser, Phys. Rev. Lett. **24**, 1041 (1970).
- ²N. Boccara, R. Mejdani, and L. de Seze, J. de Phys. **7**, 149 (1977).
- ³D. K. Remler and A. D. J. Haymet, J. Phys. Chem. **90**, 5426 (1986).
- ⁴R. Rosso, Liquid Crystals **34**, 737 (2007).

- ⁵R. Berardi, L. Muccioli, S. Orlandi, M. Ricci, and C. Zannoni, *J. Phys.: Condensed Matter* **20**, 463101 (2008).
- ⁶G. R. Luckhurst, *Nature* **430**, 413 (2004).
- ⁷L. A. Madsen, T. J. Dingemans, M. Nakata, and E. T. Samulski, *Phys. Rev. Lett.* **92**, 145505 (2004).
- ⁸B. R. Acharya, A. Primak, and S. Kumar, *Phys. Rev. Lett.* **92**, 145506 (2004).
- ⁹L. J. Yu and A. Saupe, *Phys. Rev. Lett.* **45**, 1000 (1980).
- ¹⁰V. Görtz and J. W. Goodby, *Chem. Commun.* , 3262 (2005).
- ¹¹B. Senyuk, H. Wonderly, M. Mathews, Q. Li, S. V. Shiyankovskii, and O. D. Lavrentovich, *Phys. Rev. E* **82**, 041711 (2010).
- ¹²Y. K. Kim, M. Majumdar, B. I. Senyuk, L. Tortora, J. Seltmann, M. Lehmann, A. Jákli, J. Gleeson, O. D. Lavrentovich, and S. Sprunt, *Soft Matter* **8**, 8880 (2013).
- ¹³A. Galindo, A. J. Haslam, S. Varga, G. Jackson, A. Vanakaras, D. J. Photinos, and D. Dunmur, *J. Chem. Phys.* **119**, 5216 (2003).
- ¹⁴P. I. C. Teixeira, M. A. Osipov, and G. R. Luckhurst, *Phys. Rev. E* **73**, 061708 (2006).
- ¹⁵M. Matsushita, *Mol. Cryst. Liq. Cryst.* **68**, 949 (1981).
- ¹⁶T. Hegmann, J. Kain, S. Diele, G. Pelzl, and C. Tschierske, *Angew. Chem. Int. Ed.* **40**, 887 (2001).
- ¹⁷K. Kaznacheev and T. Hegmann, *Phys. Chem. Chem. Phys.* **9**, 1705 (2007).
- ¹⁸C. V. Yelamaggad, S. K. Prasad, G. G. Nair, I. S. Shashikala, D. S. S. Rao, C. V. Lobo, and S. Chandrasekhar, *Angew. Chem. Int. Ed.* **43**, 3429 (2004).
- ¹⁹Y. Wang, H. G. Yoon, H. K. Bisoyi, S. Kumar, and Q. Li, *J. Mater. Chem.* **22**, 20363 (2012).
- ²⁰A. Eremin, S. Diele, G. Pelzl, H. Nádasi, W. Weissflog, J. Salfetnikova, and H. Kresse, *Phys. Rev. E* **64**, 051707 (2001).
- ²¹R. A. Reddy, C. Zhu, R. Shao, E. Korblova, T. Gong, Y. Shen, E. Garcia, M. A. Glaser, J. E. Maclennan, D. M. Walba, and N. A. Clark, *Science* **332**, 72 (2011).
- ²²B. K. Sadashiva, R. A. Reddy, R. Pratibha, and N. V. Madhusudana, *J. Mater. Chem.* **12**, 943 (2002).
- ²³H. N. S. Murthy and B. K. Sadashiva, *Liq. Cryst.* **31**, 567 (2004).
- ²⁴C. V. Yelamaggad, I. S. Shashikala, D. S. S. Rao, G. G. Nair, and S. K. Prasad, *J. Mater. Chem.* **16**, 4099 (2006).

- ²⁵R. Berardi and C. Zannoni, *J. Chem. Phys.* **113**, 5971 (2000).
- ²⁶W. L. McMillan, *Phys. Rev. A* **4**, 1238 (1971).
- ²⁷W. L. McMillan, *Phys. Rev. A* **6**, 936 (1972).
- ²⁸G. F. Kventsel, G. R. Luckhurst, and H. B. Zewdie, *Mol. Phys.* **56**, 589 (1985).
- ²⁹G. R. Luckhurst, C. Zannoni, P. L. Nordio, and U. Segre, *Mol. Phys.* **30**, 1345 (1975).
- ³⁰A. Sonnet, E. G. Virga, and G. E. Durand, *Phys. Rev. E* **67**, 061701 (2003).
- ³¹P. G. de Gennes and J. Prost, *The Physics of Liquid Crystals*, 2nd ed. (Oxford University Press, Oxford, 1993).
- ³²J. P. Straley, *Phys. Rev. A* **10**, 1881 (1974).
- ³³M. D. Lipkin and D. W. Oxtoby, *J. Chem. Phys.* **79**, 1939 (1983).
- ³⁴S. Singh, *Phys. Rep.* **324**, 107 (2000).
- ³⁵S. Miyajima, K. Nakazawa, K. Niikura, Y. Ujiye, M. Yashiro, and T. Chiba, *Liq. Cryst* **8**, 707 (1990).
- ³⁶P. Pardhasaradhi, D. M. Latha, P. V. D. Prasad, G. P. Rani, P. R. Alapati, and V. G. K. M. Pisipati, *J. Therm. Anal. Calorim.* **11**, 1483–1490 (2013).
- ³⁷G. De Matteis, F. Bisi, and E. G. Virga, *Con. Mech. Therm.* **19**, 1 (2007).
- ³⁸G. D. Matteis and E. G. Virga, *Phys. Rev. E* **71**, 061703 (2005).
- ³⁹S. S. Turzi and T. J. Sluckin, *SIAM J. App. Math* **73**, 1139 (2013).
- ⁴⁰M. Bates and G. Luckhurst, *J. Chem. Phys.* **110**, 7087 (1999).
- ⁴¹A. Pizzirusso, M. Savini, L. Muccioli, and C. Zannoni, *J. Mater. Chem.* **21**, 125 (2011).
- ⁴²M. F. Palermo, A. Pizzirusso, L. Muccioli, and C. Zannoni, “An atomistic description of the nematic and smectic phases of 4-n-octyl-4’ cyanobiphenyl (8cb),” (2013), to be published.
- ⁴³A. Ferrarini, G. R. Luckhurst, P. L. Nordio, and S. J. Roskilly, *Liq. Cryst.* **21**, 373 (1996).
- ⁴⁴G. R. Luckhurst, in *Physical Properties of Liquid Crystals Nematics*, edited by D. A. Dunmur, A. Fukuda, and G. R. Luckhurst (INSPEC, 2001).